Journal of Biomolecular NMR, **12:** 223–230, 1998.
KLUWER/ESCOM

A new experiment for the measurement of $^{n}J(C,P)$ coupling constants including $^{3}J(C4'_i,P_i)$ and $^{3}J(C4'_i,P_{i+1})$ in oligonucleotides

Christian Richter[a], Bernd Reif[a], Karlheinz Wörner[a], Stefanie Quant[a], John P. Marino[b], Joachim W. Engels[a], Christian Griesinger[a,*] & Harald Schwalbe[a,*]
[a]*Institut für Organische Chemie, Universität Frankfurt, Marie-Curie Strasse 11, D-60439 Frankfurt am Main, Germany*
[b]*Center for Advanced Research in Biotechnology, 9600 Gudelsky Drive, Rockville, MD 20850, U.S.A.*

Received 5 December 1997; Accepted 16 January 1998

Key words: RN4 structure determination, coupling constants, ^{13}C block labelled RNA, chemical synthesis

Abstract

A new experiment for the measurement of $^{n}J(C,P)$ coupling constants along the phosphodiester backbone in RNA and DNA based on a quantitative-J HCP experiment is presented. In addition to coupling constants, in which a carbon atom couples to only one phosphorus atom, both the intraresidual $^{3}J(C4'_i,P_i)$ and the sequential $^{3}J(C4'_i,P_{i+1})$ for the C4′ resonances that couple to two phosphorus atoms can be obtained. Coupling constants obtained by this new method are compared to values obtained from the P-FIDS experiment. Together with $^{3}J(H,P)$ coupling constants measured using the P-FIDS experiment, the backbone angles β and ϵ can be determined.

The interpretation of $^{3}J(C,P)$ and $^{3}J(H,P)$ coupling constants is a valuable tool to restrain the backbone conformation of oligonucleotides in structure calculations based on NMR data. The development of biochemical (Batey et al., 1992; Nikonowicz and Pardi, 1992; Nikonowicz et al., 1992; Michnicka et al. 1993; Zimmer and Crothers, 1995; Smith et al., 1997) and chemical (Quant et al., 1994; Kainosho, 1997) methods to prepare isotopically labelled RNA and DNA molecules has opened the possibility to determine these coupling constants in sizeable oligonucleotides. The P-FIDS (Schwalbe et al., 1993, 1994) and J-modulated CT-HSQC methods (Vuister et al., 1993, 1994; Legault et al., 1995) have been introduced to measure J(C,P) and J(H,P) coupling constants quantitatively in oligonucleotides. These methods allowed the measurement of the coupling constants $^{3}J(H3'_i,P_{i+1})$, $^{3}J(C2'_i,P_{i+1})$ around the angle ϵ and $^{3}J(H5'_i,P_i)$, $^{3}J(H5''_i,P_i)$ around the angle β. The precision and accuracy of oligonucleotide structure calculations can be improved, however, if $^{3}J(C4'_i,P_i)$ and $^{3}J(C4'_i,P_{i+1})$ coupling constants can be obtained, because they are the largest coupling constants around β and ϵ in canonical A-form RNA (Sänger, 1984; van de Ven and Hilbers, 1988). Since the C4′ carbon couples to two phosphorus atoms, coupling constants cannot be extracted from either P-FIDS or J-modulated CT-HSQC methods. In this communication, we introduce a quantitative (Bax et al., 1992; Blake et al., 1992) HCP experiment (Heus et al., 1994; Marino et al., 1994a) to determine J(C,P) coupling constants and compare the results obtained with this new method with data obtained from the P-FIDS experiment. The method is applied to a 10-mer RNA 5′-CGC**UUUU**GCG-3′, in which the carbon atoms in the ribosyl ring of all uridine nucleotides were ^{13}C labelled (Quant et al., 1994; Wörner, 1997).

$^{n}J(C,P)$ coupling constants can be obtained from a quantitative evaluation of the cross peaks in an HCP experiment by comparing the cross peak volumes to the cross peak volumes obtained in a 2D reference experiment, as shown in Figure 1. For a ^{13}C resonance that couples to only a single ^{31}P, the cross peak intensity I_{CP} is proportional to $\sin^2(\pi J(C,P)\tau_{CT})$ in the HCP experiment and $I_{ref} = \cos^2(\pi J(C, P)\tau_{CT})$ in the

* To whom correspondence should be addressed.

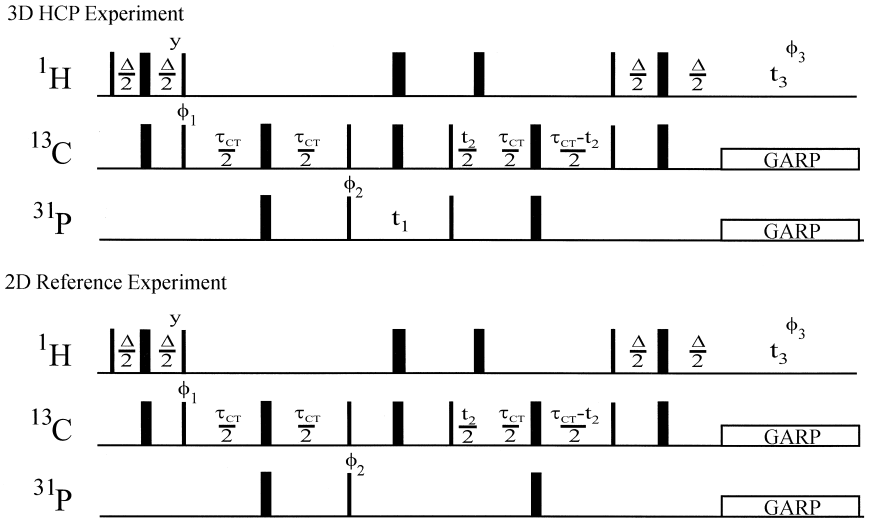

Figure 1. Pulse sequence for the 2D reference and 2D or 3D quantitative HCP experiment. Narrow and wide bars denote 90° and 180° pulses, respectively. The default phase is x. Sign discrimination in the t_1 and t_2 dimensions is obtained by altering ϕ_1 and ϕ_2 in the States-TPPI manner (Marion et al., 1989). $\Delta = 3.2$ ms, $\tau_{CT} = 25$ ms. ^{13}C and ^{31}P decoupling during acquisition are applied with 2.5 and 1.7 kHz field strength, respectively. In the 3D experiment, four scans per t_1 (32 complex points, spectral width: 800 Hz) t_2 (52 complex points, folded spectral width: 2110 Hz) experiment were recorded with 512 complex points in t_3 (spectral width: 4000 Hz). A recycle delay of 1.5 s was used, the total measurement time for the 3D experiment was 12 h on a BRUKER DRX600 equipped with a H,C,F,P QXI probe with z-gradients. The 2D reference and transfer experiments differ by the phase cycling on the receiver. In the 3D HCP, ϕ_1 = x,−x, ϕ_2 =x,x,−x,−x, ϕ_3 = x,−x,−x,x; in the 2D reference experiment, ϕ_1 =x,x,−x,−x, ϕ_3 =x,−x,x,−x. Pulse sequences can be obtained upon request from hs@org.chemie.uni-frankfurt.de.

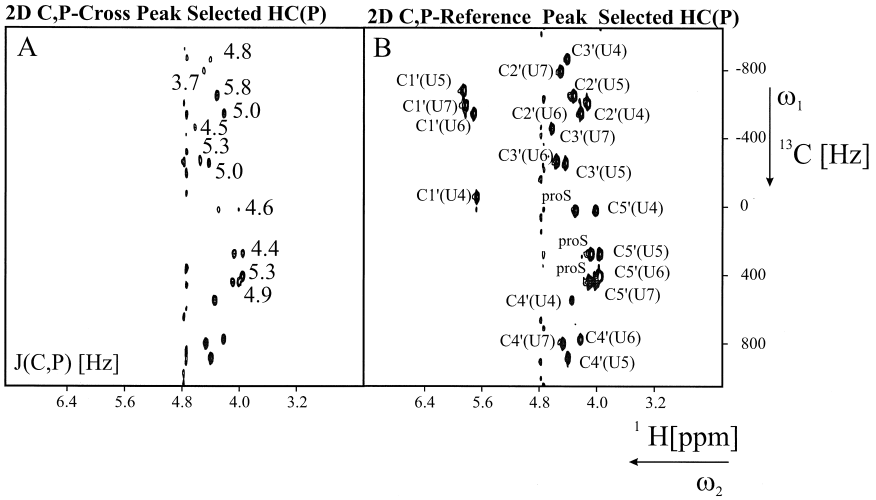

Figure 2. 2D cross peak selected (A) and reference peak selected (B) HC(P) experiment of a 1.5 mM sample of 5′-CGC**UUUU**GCG-3′ in D_2O, 100 mM NaCl, 20 mM phosphate buffer (300 µl in a Shigemi microtube). The coupling constants $^2J(C3'_i,P_{i+1})$, $2J(C5'_i,P_i)$ and $^3J(C2'_i,P_{i+1})$, together with the resonance assignments and stereospecific assignments for the pro-S H5″, are given in the figure. Squared cosine apodisation was used after zero-filling once in the ω_2 and ω_1 dimensions and linear prediction in ω_1 to double the number of complex points.

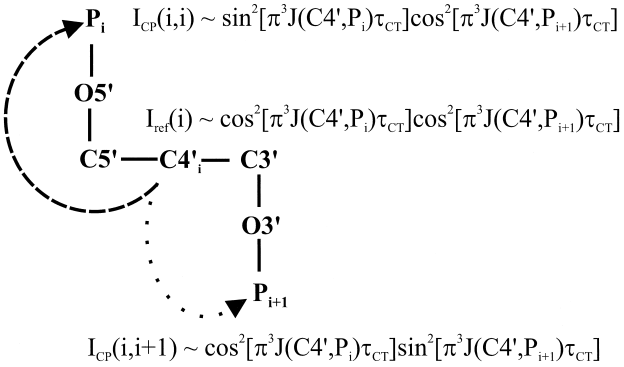

Figure 3. The cross peak intensities in the 3D HCP experiment for the $H4'_i,C4'_i,P_i$ (to the 5′ end) $I_{CP}(i,i)$ measured at $\omega_1(P_i)$ and the $H4'_i,C4'_i,P_{i+1}$ (to the 3′ end) $I_{CP}(i,i+1)$ measured at $\omega_1(P_{i+1})$ and the reference peak $I_{ref}(i)$ in the 2D reference experiment.

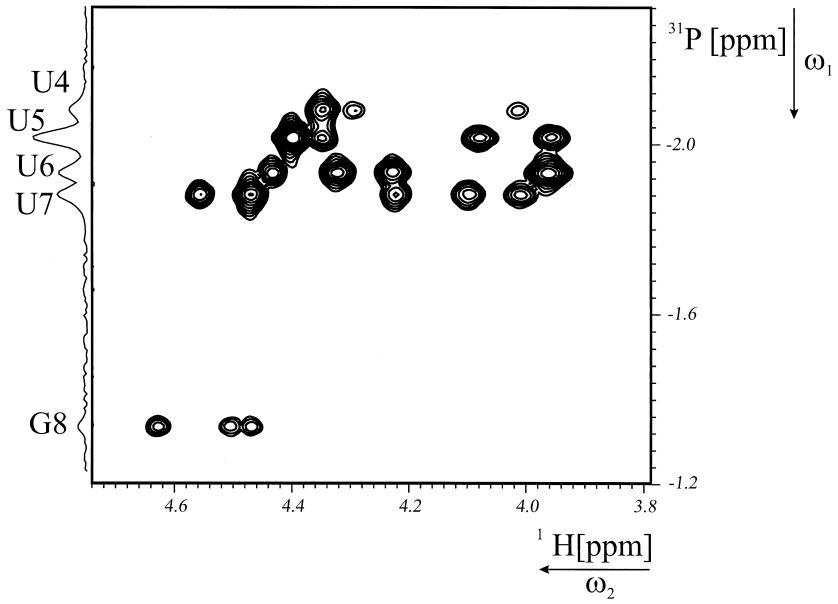

Figure 4. H, P projection from the 3D HCP showing the ^{31}P resolution of the 10-mer 5′-CGC**UUUU**GCG-3′. Squared cosine apodisation was used after zero-filling once in the ω_3, ω_2 and ω_1 dimensions and forward linear prediction in the ^{31}P dimension to double the number of complex points. Weak cross peak intensities for the $H5'_i$-$C5'_i$-P_i and $H5''_i$-$C5'_i$-P_i cross peaks for U4 are also observed in a CT-HSQC.

2D reference experiment. The coupling is then given by Equation (1):

$$J(C, P) = \frac{1}{\pi\tau_{CT}} \operatorname{arctg}\sqrt{\left(\frac{I_{CP}}{I_{ref}}\right)} \qquad (1)$$

where τ_{CT} is the period during which the coupling evolves.

Figure 2 shows the two-dimensional H,C-plane of the HCP experiment of 5′-CGC**UUUU**GCG-3′. The ^1H,^{13}C correlations in this selectively labelled RNA are well resolved and the coupling constants $^2J(C3'_i,P_{i+1})$, $^3J(C2'_i,P_{i+1})$, $^3J(C2'_i,P_{i+1})$ and $^2J(C5'_i,P_i)$ (nomenclature according to IUPAC, Sänger, 1984) for the four uridine nucleotides could be extracted according to Equation (1). The coupling constants using this new method agree within 0.3–1.0 Hz to values obtained from a P-FIDS experiment (see Table 1).

For ^{13}C nuclei that couple to two ^{31}P nuclei such as the C4′, the P-FIDS, J-modulated CT-HSQC and a *two-dimensional* quantitative HCP method all fail to provide individual $^3J(C4',P)$ coupling constants because the two coupling constants cannot be disentangled from the measurable cross peaks in the HC-(P). However, thes coupling constants can be obtained from the 3D version of the HCP by quantifying the observed individual correlations of C4′

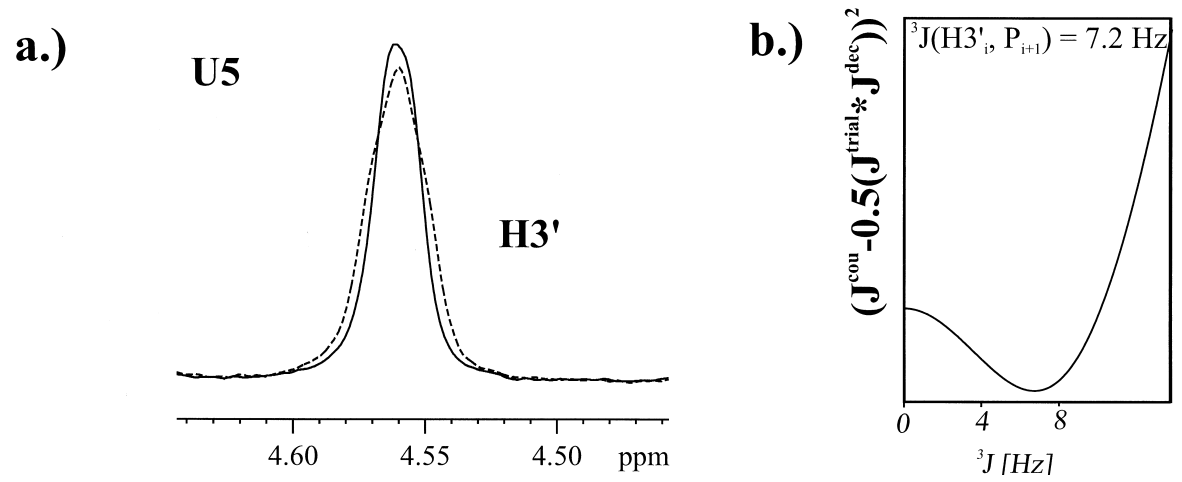

Figure 5. (a) Experimental 1D rows from the P-FIDS experiment (Schwalbe et al., 1994) with (solid line) and without (dashed line) ^{31}P decoupling during acquisition for H3′ resonances for residue U5. The broadening of the coupled (dashed) multiplet is clearly visible. (b) Fitting of the coupling of interest in a one-parameter fit gives a coupling of 7.2 Hz for ^{3}J(H3′$_i$, P$_{i+1}$).

to both the intra- and interresidual ^{31}P nuclei. In the 3D version of the HCP the cross peak intensity of the H4′$_i$,C4′$_i$,P$_i$ correlation I_{CP}(i,i), is proportional to $\sin^2(\pi^3J(C4'_i, P_i)\tau_{CT})\cos^2(\pi^3J(C4'_i, P_{i+1})\tau_{CT})$ and the cross peak intensity of the H4′$_i$,C4′$_i$,P$_{i+1}$ correlation, I_{CP}(i,i+1), is proportional to $\cos^2(\pi^3J(C4'_i, P_i)\tau_{CT}$ $\sin^2(\pi^3J(C4'_i, P_{i+1})\tau_{CT})$. The intensity of the H4′,C4′ correlation I_{ref}(i) in the 2D reference experiment is proportional to $\cos^2(\pi^3J(C4'_i, P_i)\tau_{CT})\cos^2(\pi^3J(C4'_i, P_{i+1})\tau_{CT})$ (see Figure 3). The two desired ^{3}J coupling constants can be derived from Equation (2):

$$J(C4'_i, P_i) = \frac{1}{\pi\tau_{CT}}\,\mathrm{arctg}\sqrt{\left(\frac{I_{CP}(i,i)}{I_{ref}(i)}\right)}$$

$$J(C4'_i, P_{i+1}) = \frac{1}{\pi\tau_{CT}}\,\mathrm{arctg}\sqrt{\left(\frac{I_{CP}(i,i+1)}{I_{ref}(i)}\right)} \quad (2)$$

While the cross peaks have to be extracted from a 3D experiment, the reference intensity can only be extracted from a 2D experiment and therefore, intensities obtained from experiments with different overall measurement time have to be compared. Similar approaches for the measurement of ^{3}J(N,C$^\gamma$) in a protein have been obtained by Konrat et al. (1997) and Hu et al. (Hu and Bax, 1997; Hu et al., 1997). The following procedure for the quantification of the cross peak and the reference peak has been applied in this communication.

For both the 2D reference and the 3D experiment, a 3D Fourier transformation has been applied. The 2D data set was copied to yield the real part of the ^{31}P spectrum, while the imaginary part was set to 0. A 3D Fourier transformation of the reference experiment then yields a spectrum with peaks at the $\omega_1(^{31}P) = 0$ frequency. Coupling constants for e.g. a J(C4′$_i$,P$_i$) are then given by:

$$\frac{I_{CP}}{I_{ref}} = \frac{NS_{CP}}{NS_{ref}}\,\tan^2\,(\pi^3J(C4'_i, P_i)\tau_{CT}) \quad (3)$$

Alternatively, a calibration constant can be obtained from already determined coupling constants of carbons coupled to only one ^{31}P. Both procedures gave the same results. Figure 4 shows a H,P-projection from the 3D HCP experiment with marked H4′,P cross peaks and the extracted coupling constants.

The tree staggered rotamers around β and ϵ are shown in Figure 5 together with the theoretical coupling constants taking the parametrisations for ^{3}J(C,P) and ^{3}J(H,P) by Lankhorst et al. (1984). All ^{3}J(C4′$_i$,P$_i$) coupling constants are large, indicating a conformation close to 180° for β. This is further supported by the small ^{3}J(H5′$^{proR}_i$,P$_i$) and ^{3}J(H5″$^{proS}_i$,P$_i$) coupling constants for all U residues except U6, where the two H5′ proton resonances overlap (see Table 1). For a more precise determination of the angle β, the diastereotopic H5′, H5″ protons need to be assigned stereospecifically. This has been achieved from measurement of ^{2}J(H5′$^{proR}_i$,C4′$_i$) and ^{2}J(H5″$^{proS}_i$,C4′$_i$) coupling constants derived in a C5′,H5′ selective HSQC (Marino et al., 1996) and from ^{3}J(H5′$^{proR}_i$,H4′$_i$) and ^{3}J(H5″^{proS}$_i$,H4′$_i$) (see Table 1) measured in the forward-directed HCC-TOCSY-CCH-E.COSY (Schwalbe et al., 1995). With

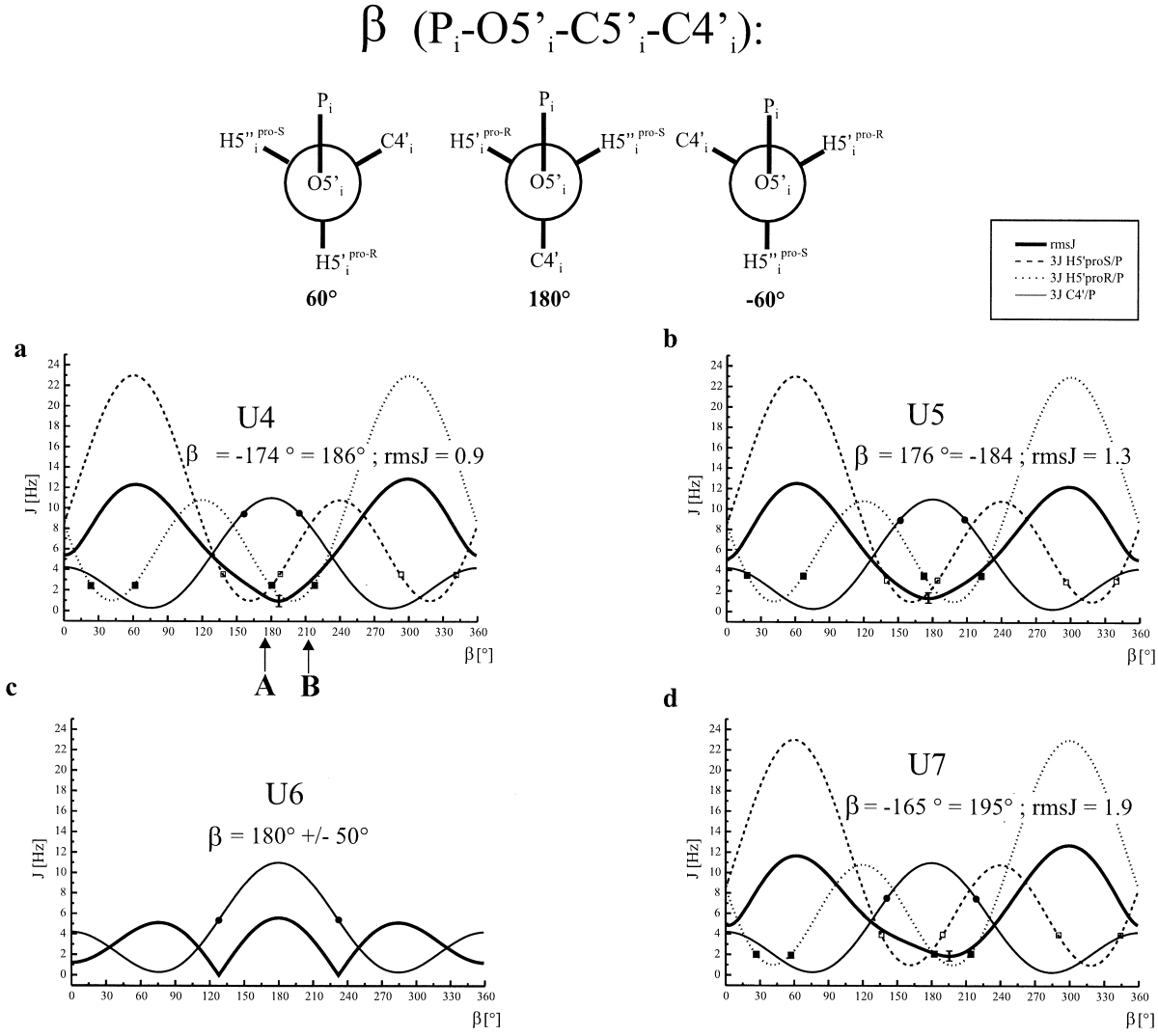

Figure 6. Coupling constants around the backbone angle β: (a–d) Theoretical Karplus curves (as lines) and experimental values (data points), respectively, for: – – – ^{3}J(H5″$_i^{proS}$,P$_i$), □; · · · ^{3}J(H5′$_i^{proR}$, ■; — ^{3}J(C4′$_i$, P$_i$), ●. The coupling constants were calculated using the calibration of Lankhorst et al. (1988): $^3J(C, P) = 6.9\cos^2\phi - 3.4\cos\phi + 0.7$; $^3J(H, P) = 15.3\cos^2\phi - 6.1\cos\phi + 1.6$. The rmsJ in dependence of β (—) for a fit to a single conformation is shown. Unique minima are found for a, b, d and e. The staggered rotamers are shown at the top as well as the β values for canonical A-form RNA (A) and B-form DNA (B). The standard deviation of coupling constants measured in three different experiments is indicated as a vertical error bar on the rmsJ curve.

the stereospecific assignments, the rmsJ curves for β (Figure 6a–d)) that are asymmetric with respect to reflection about $\beta = 180°$ have been obtained.

The conformational analysis for the angle ϵ is more complex. While all four uridine residues are close to a staggered canonical rotamer $\beta = 180°$, a variation of angles is observed around the angle ϵ. The analysis of coupling constants for U4 is in agreement with an angle $\epsilon = -146°$, close to the canonical A-form angle of $-151°$ (Sänger, 1984). For U5, U6, and U7, taking the parametrisations by Lankhorst et al. derived from temperature-dependent coupling constant measurements on small oligonucleotides, we find for fitting to a single conformation an angle $\epsilon \sim 125°$, which is close, but not identical to the angles of 155° observed for B-form helices. As can be seen in Figures 7a–d, the rmsJ is also near the minimum values for an eclipsed conformation with $\epsilon \sim 0°$, which cannot be excluded on the basis of coupling constant data alone (Table 2). Fitting the data to a two-state model

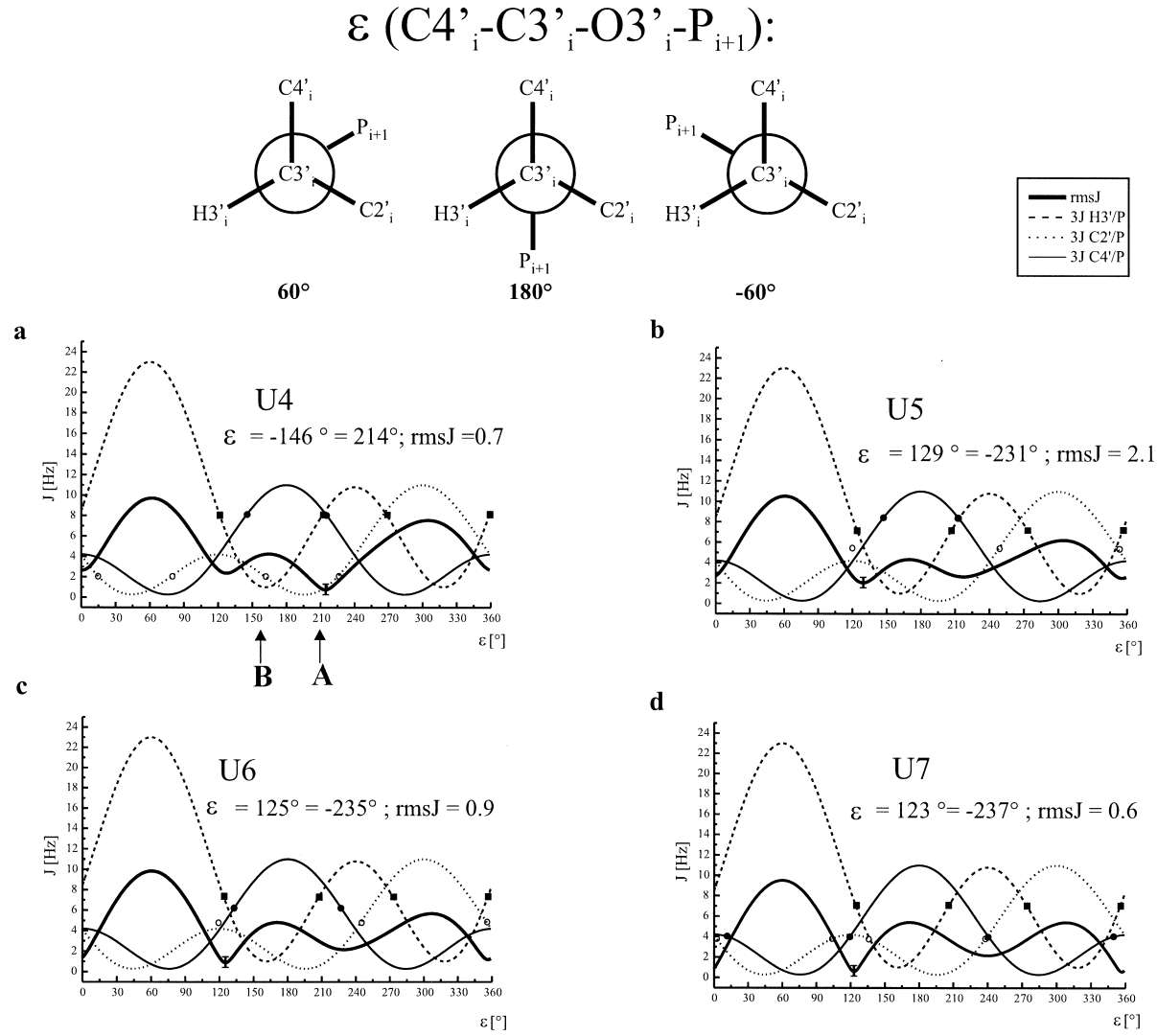

Figure 7. Coupling constants around the backbone angle ϵ: (a–d) Theoretical Karplus curves (as lines) and experimental values (data points), respectively, for : – – – ^{3}J($H3'_{i}$,P_{i+1}), ■; ··· ^{3}J($C2'_{i}$,P_{i}), ○; — ^{3}J($C4'_{i}$,P_{i+1}), ●. The rmsJ in dependence of ϵ (—) for a fit to a single conformation is shown. The staggered rotamers are shown at the top as well as ϵ values for canonical A-form RNA (A) and B-form DNA (B). The standard deviation of coupling constants measured in three different experiments is indicated as a vertical error bar on the rmsJ curve.

with fixed ϵ values found in canonical A- and B-form RNA (−151°, 155°, respectively), no significant improvement is found. Fitting to a two-state model with two free angles for ϵ, eclipsed rotamers are found as predominant rotamers. On the basis of the coupling constant data alone, we are not in a position to exclude conformational averaging and a single, non-canonical conformation around ϵ. We are in the process of structure calculation using additional experimental torsion angle restraints and a quantitative analysis of the NOE data to address this problem.

For the determination of ^{3}J(C4′,P), the $C4'_{i}$,P_{i} and $C4'_{i}$,P_{i} and $C4'_{i}$,P_{i+1} cross peaks in the 3D HCP experiment need to be resolved. In cases in which either of the two correlations overlap with C4′,P cross peaks of other residues, as may be likely in larger molecules, further correlation steps, e.g. like proposed in the HCP-CCH-TOCSY (Marino et al., 1994b; Wijmenga et al., 1995), will be needed to achieve better resolution. If the sequential cross peaks for a single residue mutually overlap, cross peak integration will yield:

Table 1. ^{3}J(H,P) and ^{3}J(C,P) coupling constants and backbone angles.

	Residue Coupling	U4	U 5	U6	U7
β	$^3J(H5'^{proS}_i,P_i)$[a,b]	3.6	3.0	[d]	4.0
	$^3J(H5'^{proR}_i,P_i)$	2.5	3.5	[d]	2.1
	$^3J(C4'_i,P-i)$	9.5[c]	9.0	5.4	7.5
γ	$^3J(H5'^{proS}_i,H4'_i)$[e,f]	1.9	2.0	[d]	1.0
	$^3J(H5'^{proR}_i,H4'_i)$	3.3	4.3	[d]	1.7
	$^2J(H5'^{proS}_i,C4'_i)$	−3.5	−4.7	[d]	−2.4
	$^2J(H5'^{proR}_i,C4'_i)$	−1.0	0.4	[d]	−1.5
ϵ	$^3J(J3'_i,P_{i+1})$	8.1	7.2	7.4	7.1
	$^3J(C2'_i,P_{i+1})$	2.2[c]	5.4	4.8	3.8
		2.1[g]	6.0	5.1	3.8
		2.7[h]	6.6	6.0	3.7
	$^3J(C4'_i,P_{i+1})$	8.4[c]	8.5	6.2	3.8
	$^2J(C3'_i,P_{i+1})$	6.4[c]	5.0	5.2	4.4
		4.8[g]	5.0	5.3	4.5
		5.2[h]	5.1	5.0	5.0
	$^2J(C5'_i,P_i)$	4.3± 0.3[c,i]	4.9 ± 0.5	5.2[d]	5.5 ± 0.7
		4.6[g]	4.4	5.3	4.9
		5.1[h]	5.3	–	5.6
Backbone angle					
	β, rmsJ[j]	−174° 0.9	176° 1.3	180°[k] ± 50°	−165° 1.9
	ϵ, rmsJ[j]	−146° 0.7	129° 0.9	125° 0.9	123° 0.6

[a] Measured in Hz.
[b] Measured in PFIDS experiment in ω_2 (see Figure 5).
[c] From 3D quantitative HCP.
[d] Overlapped.
[e] Measured in HCC-TOCSY-CCH-E.COSY (Schwalbe et al., 1995).
[f] Stereospecific assignments from C5′,H5′-selective HSQC (Marino et al., 1996).
[g] From 2D quantitative HCP.
[h] Values parenthesis from PFIDS experiment in ω_1.
[i] Average between $H5'^{proS}$ and $H5'^{proR}$.
[j] $rmsJ = (\sum(J_{pred}{}^2 - J_{exp}{}^2))^{-1/2}/(n)^{-1/2}$ measured in Hz, n number of couplings, theoretical J calculation for J(C,P) and for J(H,P) parametrisations (Lankhorst et al., 1984).
[k] Based on the observation of only $^3J(C4'_i,P_i)$.

$$\sin^2(\pi^3J(C_i, P_i)\tau_{CT})\cos^2(\pi^3J(C_i, P_{i+1})\tau_{CT}) + \cos^2(\pi^3J(C_i, P_i)\tau_{CT})\sin^2(\pi^3J(C_i, P_{i+1})\tau_{CT}) = \sin^2((\pi^3J(C_i, P_i) + \pi^3J(C_i, P_{i+1}))\tau_{CT}) \quad (4)$$

and therefore only the sum of the coupling $^3J(C4'_i,P_i)$and $^3J(C4'_i,P_i)$
and $^3J(C4'_i,P_{i+1})$ can be determined. In this respect, the availability of selectively labelled oligonucleotides prepared by chemical solid phase synthesis may be of advantage. Furthermore, for larger oligonucleotides the sensitivity may drop in the rather long CT periods on carbon. However, sensitivity improvement techniques (Marino et al., 1997; Pervushin et al., 1997) with greatly improved relaxation properties may substitute the experiments based on evolution of single quantum coherences proposed here.

^{3}J(C,P) coupling constants can be determined with high accuracy from quantitative analysis of a 3D HCP experiment and a 2D reference experiment. It is shown that quantification of a 3D HCP yields both $^3J(C4'_i,P_i)$ and $^3J(C4'_i,P_{i+1})$ coupling constants. Conformational analysis shows the potential of additional coupling constant data together with J(H,P) coupling constants from PFIDS experiments to better define the backbone angles β and ϵ.

Table 2. Different conformational models to fit experimental coupling constants

Residue Backbone angle	U4	U5	U6	U7
Model I, fixed ϵ				
ϵ, rmsJ[a]	$-146°$ 0.7	$129°$ 2.1	$125°$ 0.9	$123°$ 0.6
Model II				
$\epsilon = 151°, 155°$, $\%\epsilon^{155°}$	100% 1.2	76% 2.7	83% 2.9	85% 3.6
Model III				
ϵ_1, ϵ_2, $\%\epsilon_1$	$0° \quad -145° \quad 74\%$	$0° \quad -62° \quad 79\%$	$0° \quad -5° \quad 69\%$	$124° \quad -3° \quad 41\%$
rmsJ	0.4	0.1	0.1	0.5
Model IV				
$\epsilon = 60°, 180°, -60°$ %	26, 67, 7	18, 50, 26	22, 46, 32	25, 38, 37
rmsJ	0.7	1.8	0.7	0.7

[a] $\text{rmsJ} = (\sum(J_{pred}{}^2 - J_{exp}{}^2))^{-1/2}/(n)^{-1/2}$ measured in Hz, n number of couplings, parametrisation for J(H,P) and J(C,P) from Lankhorst et al. (1984).

The approach reported here can also be applied in proteins to simultaneously determine $^1J(N_i,C_i^\alpha)$ and $^2J(N_i,C_{i-1}^\alpha)$ coupling constants from 2D reference and 3D HNCA experiments.

Acknowledgements

This work was supported by the DFG (Gr1211/2–4 and En111/11-1). Spectra were acquired at the 'Large Scale Facility for Biomolecular NMR' at the University of Frankfurt am Main H.S. acknowledges a fellowship from the European Large Scale Facility.

References

Batey, R.T., Inada, M., Kujawinski, E., Puglisi, J.D. and Williamson, J.R. (1992) *Nucleic Acids Res.*, **20**, 4515–4523.

Bax, A., Max, D. and Zax, D. (1992) *J. Am. Chem. Soc.*, **114**, 6924–6925.

Blake, P.R., Lee, B. Summers, M.F., Adams, M.W.W., Park, J.-B., Zhou, Z.H. and Bax, A. (1992) *J. Biomol. NMR*, **2**, 527–533.

Heus, H.A., Wijmenga, S.S., van de Ven, F.J.M. and Hilbers, C.W. (1994) *J. Am. Chem. Soc.*, **116**, 4983–4984.

Hu, J.-S. and Bax, A. (1997) *J. Biomol. NMR*, **9**, 323–328.

Hu, J.-S., Grzesiek, S. and Bax, A. (1997) *J. Am. Chem. Soc.*, **119**, 1803–1804.

Kainosho, M. (1997) *Nat. Struct. Biol.*, **4**, 858–861, and references cited therein.

Konrat, R., Muhandiram, D.R., Farrow, N.A. and Kay, L.E. (1997) *J. Biomol. NMR*, **9**, 409–422.

Lankhorst, P.P., Haasnoot, C.A.G., Erkelens, C. and Altona, C. (1984) *J. Biomol Struct. Dyn.*, **1**, 1387–1405.

Legault, P., Jucker, F.M. and Pardi, A. (1995) *FEBS Lett.*, **362**, 156–160.

Marino, J.P., Schwalbe, H., Anklin, C., Bermel, W., Crothers, D.M. and Griesinger, C. (1994a) *J. Am. Chem. Soc.*, **116**, 6472–6473.

Marino, J.P., Schwalbe, H., Anklin, C., Bermel, W., Crothers, D.M. and Griesinger, C. (1994b) *J. Biomol. NMR*, **5**, 87–92.

Marino, J.P., Schwalbe, H., Glaser, S.J. and Griesinger, C. (1996) *J. Am. Chem. Soc.*, **118**, 4388–4395.

Marino, J.P., Diener, J.L., Moore, P.B. and Griesinger, C. (1997) *J. Am. Chem. Soc.*, **119**, 7361–7366.

Marion, D., Ikura, M., Tschudin, R. and Bax, A. (1989) *J. Magn. Reson.*, **85**, 393–399.

Michnicka, M.J., Harper, J.W. and King, G.C. (1993) *Biochemistry*, **32**, 395–400.

Nikonowicz, E.P. and Pardi, A. (1992) *Nature*, **335**, 184–186.

Nikonowicz, E.P., Sirr, A., Legault, P., Jucker, F.M., Baer, L.M. and Pardi, A. (1992) *Nucleic Acids Res.*, **20**, 4507–4513.

Pervushin, K., Riek, R., Wider, G. and Wüthrich, K. (1997) *Proc. Natl. Acad. Sci. USA*, **94**, 12366–12371.

Quant, S., Wechselberger, R.W., Wolter, M.A., Wörner, K.-H., Schell, P., Engels, J.W., Griesinger, C. and Schwalbe, H. (1994) *Tetrahedron Lett.*, **35**, 6649–6652.

Sänger, W. (1984) *Principles of Nucleic Acid Structure*, 2nd ed., Springer, New York, NY.

Schwalbe, H., Samstag, W., Engels, J.W., Bermel, W. and Griesinger, C. (1993) *J. Biomol. NMR*, **3**, 479–486.

Schwalbe, H., Marino, J.P., King, G.C., Wechselberger, R., Bermel, W. and Griesinger, C. (1994) *J. Biomol. NMR*, **4**, 631–644.

Schwalbe, H., Marino, J.P., Glaser, S.J. and Griesinger, C. (1995) *J. Am. Chem. Soc.*, **117**, 7251–7252.

Smith, D.E., Su, J.-Y. and Jucker, F.M. (1997) *J. Biomol. NMR*, **10**, 245–254.

van de Ven, F.J.M. and Hilbers, C.W. (1988) *Eur. J. Biochem*, **178**, 1.

Vuister, G.W., Wang, A.C. and Bax, A. (1993) *J. Am. Chem. Soc.*, **115**, 5334–5335.

Vuister, G.W., Grzesiek, S., Delaglio, F., Wang, A.C., Tschudin, R. and Bax, A. (1994) *Methods Enzymol.*, **239**, 79–105 and references cited therein.

Wijmenga, S.S., Heus, H.A., Leeuw, H.A., Hoppe, H., van der Graaf, M. and Hilbers, C.W. (1995) *J. Biomol. NMR*, **5**, 82–86.

Wörner, K. (1997) Ph.D. Thesis, University Frankfurt am Main.

Zimmer, D.P. and Crothers, D.M. (1995) *Proc. Natl. Acad. Sci. USA*, **92**, 3091–3095.